Pergamon

Geochimica et Cosmochimica Acta, Vol. 67, No. 24, pp. 4775–4789, 2003

0016-7037/03 $30.00 + .00

doi:10.1016/S0016-7037(03)00310-7

Petrogenesis of angrites

CHRISTINE FLOSS,[1,*] GHISLAINE CROZAZ,[1] GORDON MCKAY,[2] TAKASHI MIKOUCHI,[3] and MARVIN KILLGORE[4]

[1]Laboratory for Space Sciences and Department of Earth and Planetary Sciences, Washington University, St. Louis, MO 63130, USA
[2]Mail Code SN2, NASA Johnson Space Center, Houston, TX 77058, USA
[3]Department of Earth and Planetary Science, University of Tokyo, Hongo Bunkyo-ku, Tokyo 113-0033, Japan
[4]Southwest Meteorite Laboratory, P.O. Box 95, Payson, AZ 85547, USA

(*Received December* 12, 2002; *accepted in revised form May* 2, 2003)

Abstract—The recent discovery of two new angrites, Sahara 99555 and D'Orbigny, has revived interest in this small group of achondrites. We measured trace element abundances in the individual minerals of these two angrites and compared them with the three Antarctic angrites, LEW 86010, LEW 87051 and Asuka 881371. Trace element variations in four of these meteorites (LEW 87051, Asuka 881371, Sahara 99555 and D'Orbigny) indicate rapid crystallization under near closed system conditions, consistent with their mineralogical and textural features. All four appear to be closely related and crystallized from very similar magmas. Discrepancies between their bulk REE compositions and melts calculated to be in equilibrium with the major phases may be due in part to kinetic effects of rapid crystallization. Prior crystallization of olivine and/or plagioclase may also account for the elevated parent melt composition of clinopyroxene in some of the angrites such as Asuka 881371.

LEW 86010 also crystallized from a melt and represents a liquid composition, but trace element trends in clinopyroxene and olivine differ from those of the other angrites. This meteorite seems to have crystallized from a different source magma. *Copyright © 2003 Elsevier Ltd*

1. INTRODUCTION

The angrites are a small group of achondrites characterized by unusual mineral assemblages and refractory element enrichments. In addition to their exotic compositions, these meteorites have unusually old ages. One of the notable features of the original angrite, Angra dos Reis, is its very primitive initial $^{87}Sr/^{86}Sr$ ratio that is distinctly below that of basaltic achondrites (BABI), indicating that it formed shortly after condensation of the first solids in the solar system (Wasserburg et al., 1977). Sm-Nd and Pb-Pb dating also confirm its old age (~4.55 Ga), as does the presence of ^{244}Pu-induced fission xenon (Lugmair and Marti, 1977; Störzer and Pellas, 1977; Wasserburg et al., 1977). Chronological studies of LEW 86010 and Asuka 881371, including Sm-Nd, Pb-Pb, Mn-Cr and Rb-Sr systematics (e.g., Lugmair and Galer, 1992; Nyquist et al., 1994; Premo and Tatsumoto, 1995) indicate that these angrites are contemporaneous with Angra dos Reis.

Research on the angrites (e.g., Prinz et al., 1977; Mittlefehldt and Lindstrom, 1990; Crozaz and McKay, 1990; McKay et al., 1994; Mikouchi et al., 1996) has been hampered by the fact that since the 1980s, they have been represented by only four meteorites, Angra dos Reis (AdoR), which gave its name to the group, and the Antarctic angrites, LEW 86010 (LEW86), LEW 87051 (LEW87) and Asuka 881371 (A88), the latter three with a combined mass of only 18.5 g. This situation has changed recently with the discovery of two new angrites, Sahara 99555 (S99) and D'Orbigny (DOR), with masses of 2.7 and 16.6 kg, respectively. Not only did the recovery of these meteorites significantly increase the amount of material available for study, but it has also offered, for the first time in a decade, the opportunity to obtain new information about the petrogenesis of the angrites (e.g., Mittlefehldt et al., 2002). Moreover, the existence of a seventh angrite has recently been reported (Jambon et al., 2002).

Angra dos Reis is dominated by megacrysts of the clinopyroxene Al-Ti-diopside-hedenbergite (formerly known as fassaite) and has generally been interpreted as an annealed magmatic cumulate (e.g., Prinz et al., 1977), although other interpretations have also been suggested (Treiman, 1989). All other angrites, including Sahara 99555 and D'Orbigny, have igneous (granular or basaltic) textures and contain abundant olivine (including kirschsteinite) and anorthite in addition to clinopyroxene (McKay et al., 1995a; Mikouchi et al., 2000a; Kurat et al., 2001a, 2001b; Mikouchi and McKay, 2001). Geochemical data further emphasize the distinct nature of Angra dos Reis. Crozaz and McKay (1990) carried out detailed trace element analyses of individual minerals from Angra dos Reis and LEW 86010 and concluded that, despite common characteristics, the two meteorites must have been produced in separate magmatic events. Mittlefehldt and Lindstrom (1990) also noted the distinctiveness of Angra dos Reis, and suggested that either the angrite parent body was heterogeneous or this meteorite formed on a separate parent body.

The remaining angrites, however, appear to be more closely related. In particular, Mikouchi et al. (2000a) and Mikouchi and McKay (2001) have noted that Sahara 99555 and D'Orbigny are texturally and mineralogically very similar to the Antarctic angrites LEW 87051 and Asuka 881371. In this work we carried out a detailed investigation of the trace element distributions of the new angrites, Sahara 99555 and D'Orbigny, and compared these data with similar measurements for the three Antarctic angrites. Preliminary data were reported by McKay et al. (1990, 1995a) and Floss et al. (2000, 2001).

* Author to whom correspondence should be addressed (floss@wuphys.wustl.edu).

Table 1. Representative elemental concentrations in plagioclase and glass.

	Plagioclase								Glass
	LEW86 (l)	LEW86 (h)	LEW87	A88 (l)	A88 (h)	S99	DOR (l)	DOR (h)	DOR
Na	156 ± 1	157 ± 1	363 ± 4	399 ± 1	246 ± 1	166 ± 1	112 ± 1	123 ± 1	107 ± 1
Mg (%)	0.02 ± 0.01	0.02 ± 0.01	0.27 ± 0.01	0.11 ± 0.01	0.12 ± 0.01	0.19 ± 0.01	0.13 ± 0.01	0.14 ± 0.01	6.0 ± 0.1
K	26 ± 1	20 ± 1	30 ± 1	15 ± 1	17 ± 1	5.6 ± 0.3	7.5 ± 0.2	14 ± 1	18 ± 1
Ca (%)	13.3 ± 0.1	13.2 ± 0.1	12.4 ± 0.1	12.9 ± 0.1	12.9 ± 0.1	12.9 ± 0.1	12.9 ± 0.1	13.1 ± 0.1	13.6 ± 0.1
Sc	2.8 ± 0.1	2.7 ± 0.1	3.6 ± 0.6	3.9 ± 0.2	4.2 ± 0.3	3.2 ± 0.3	4.7 ± 0.2	5.8 ± 0.2	56 ± 1
Ti	32 ± 1	45 ± 1	128 ± 3	52 ± 1	53 ± 1	89 ± 1	52 ± 1	63 ± 1	6,600 ± 8
V	2.0 ± 0.1	0.64 ± 0.03	9.9 ± 0.6	4.7 ± 0.1	4.1 ± 0.2	5.9 ± 0.2	4.4 ± 0.1	4.8 ± 0.1	103 ± 1
Cr	0.35 ± 0.02	0.81 ± 0.05	8.6 ± 0.6	2.2 ± 0.1	3.7 ± 0.2	2.8 ± 0.2	2.2 ± 0.1	1.8 ± 0.1	236 ± 1
Mn	90 ± 1	77 ± 1	126 ± 3	93 ± 1	103 ± 1	100 ± 1	95 ± 1	87 ± 1	2460 ± 5
Fe (%)	0.20 ± 0.01	0.17 ± 0.01	0.53 ± 0.01	0.22 ± 0.01	0.22 ± 0.01	0.41 ± 0.01	0.35 ± 0.01	0.47 ± 0.01	26.8 ± 0.1
Sr	119 ± 1	156 ± 1	125 ± 3	114 ± 1	124 ± 1	133 ± 1	132 ± 1	138 ± 1	110 ± 1
Y	0.080 ± 0.004	0.16 ± 0.01	0.52 ± 0.06	0.11 ± 0.01	0.16 ± 0.01	0.21 ± 0.02	0.27 ± 0.02	0.52 ± 0.03	24 ± 1
Zr	0.042 ± 0.007	0.055 ± 0.009	0.32 ± 0.06	0.042 ± 0.011	0.11 ± 0.02	0.066 ± 0.014	0.22 ± 0.03	0.13 ± 0.02	87 ± 1
Ba	4.6 ± 0.1	29 ± 1	7.4 ± 0.6	3.6 ± 0.2	4.8 ± 0.2	7.9 ± 0.3	6.9 ± 0.2	6.6 ± 0.2	23 ± 1
La	0.11 ± 0.01	0.21 ± 0.01	0.36 ± 0.07	0.11 ± 0.009	0.15 ± 0.02	0.23 ± 0.02	0.14 ± 0.01	0.20 ± 0.02	2.7 ± 0.1
Ce	0.23 ± 0.01	0.40 ± 0.02	0.71 ± 0.11	0.19 ± 0.02	0.27 ± 0.03	0.48 ± 0.03	0.32 ± 0.02	0.47 ± 0.03	6.8 ± 0.3
Pr	0.023 ± 0.002	0.043 ± 0.004	0.074 ± 0.020	0.031 ± 0.006	0.028 ± 0.006	0.050 ± 0.009	0.036 ± 0.005	0.048 ± 0.006	1.1 ± 0.1
Nd	0.11 ± 0.01	0.15 ± 0.01	0.23 ± 0.05	0.10 ± 0.01	0.13 ± 0.02	0.23 ± 0.03	0.15 ± 0.01	0.20 ± 0.02	5.9 ± 0.2
Sm	0.018 ± 0.004	0.039 ± 0.007	0.035 ± 0.044	b.d.	0.051 ± 0.017	0.048 ± 0.024	0.033 ± 0.011	0.054 ± 0.014	1.7 ± 0.1
Eu	0.54 ± 0.02	0.87 ± 0.03	0.50 ± 0.06	0.43 ± 0.02	0.47 ± 0.03	0.35 ± 0.03	0.48 ± 0.03	0.49 ± 0.03	0.63 ± 0.04
Gd	0.033 ± 0.004	0.039 ± 0.006	b.d.	b.d.	0.029 ± 0.013	0.023 ± 0.018	0.024 ± 0.009	0.028 ± 0.011	2.4 ± 0.2
Tb	0.0037 ± 00010	0.0037 ± 0.0013	b.d.	0.0023 ± 0.0022	0.0046 ± 0.0034	b.d.	0.0032 ± 0.0023	0.0068 ± 0.0030	0.41 ± 0.04
Dy	0.018 ± 0.002	0.031 ± 0.004	0.044 ± 0.024	0.012 ± 0.005	0.015 ± 0.008	0.014 ± 0.010	0.029 ± 0.006	0.024 ± 0.007	3.3 ± 0.1
Ho	0.0051 ± 0.0010	b.d.	0.016 ± 0.011	0.0037 ± 0.0021	0.0037 ± 0.0030	b.d.	0.0034 ± 0.0020	b.d.	0.69 ± 0.05
Er	0.0079 ± 0.0019	0.023 ± 0.004	b.d.	0.0077 ± 0.0053	b.d.	0.012 ± 0.011	0.017 ± 0.006	0.012 ± 0.006	1.9 ± 0.1
Tm	b.d.	0.0038 ± 0.0038	b.d.	b.d.	b.d.	b.d.	b.d.	b.d.	0.33 ± 0.02
Yb	b.d.	0.026 ± 0.006	0.015 ± 0.025	0.0093 ± 0.0078	0.014 ± 0.012	0.011 ± 0.017	0.019 ± 0.010	0.029 ± 0.011	1.9 ± 0.2
Lu	b.d.	0.0037 ± 0.0014	b.d.	b.d.	b.d.	b.d.	b.d.	b.d.	0.32 ± 0.03

In ppm, except as noted; b.d.: below detection; empty space: not measured; 'l' and 'h' refer to analyses with lower and higher REE concentrations, respectively.

2. EXPERIMENTAL

Trace elements were measured in individual minerals in polished thin sections of the angrites LEW 87051 (,2 and ,3), Asuka 881371, Sahara 99555 and in a thick section of D'Orbigny. In addition, although trace element data have previously been reported for individual minerals from LEW 86010 (Crozaz and McKay, 1990), we obtained a thin section (,6) of this angrite as well, to acquire additional analyses for several minerals. After initial documentation and characterization using a JEOL 840a scanning electron microscope, the REE and other trace elements were measured using the modified Cameca ims 3f at Washington University, according to established procedures (Zinner and Crozaz, 1986a). Secondary ions were sputtered from the samples surfaces using an O^- primary beam and were collected at low mass resolution, using energy filtering to remove complex molecular interferences. Simple molecular interferences are not removed by this method and were corrected for using an analysis program developed to deconvolve major molecular interferences in the mass regions K-Ca-Ti, Rb-Sr-Y-Zr and Ba-REEs (Alexander, 1994). REE concentrations were obtained by normalization to the reference element (Si for silicates and Ca for phosphates), using sensitivity factors reported by Zinner and Crozaz (1986b) and Floss and Jolliff (1998) for the REE, and by Hsu (1995) for other elements. Concentrations of the reference elements were determined by electron microprobe analysis of representative grains of the individual minerals from each meteorite. The ion probe analysis spots were carefully chosen, using an optical microscope, to avoid cracks or inclusions, and were examined afterwards to check for contamination in the third dimension. The errors reported in Tables 1 to 4 are 1σ due to counting statistics only, except for averages where they reflect the overall variance. REE abundances in the figures are normalized to the CI chondrite abundances of Anders and Grevesse (1989).

3. RESULTS

We measured the distributions of the REE and other trace elements in individual grains of olivine (including kirschsteinite), pyroxene, plagioclase and phosphate from LEW 86010, LEW 87051, Sahara 99555 and D'Orbigny. In general we measured several (~5–10) distinct grains of each phase in each meteorite and, where feasible, tried to measure both cores and rims of grains that might be expected to exhibit elemental zoning (e.g., clinopyroxene). Many analyses included the full suite of REE, but others were limited to other minor and trace elements (e.g., Sc, Ti, V, Zr, Y) and the REE, La to Pr, to obtain a more representative sampling of the trace element variations in a reasonable time frame. Representative analyses for each mineral are listed in Tables 1 to 4. Olivine/kirschsteinite and clinopyroxene show significant trace element zoning in most of the angrites and, thus, analyses with both lower and higher REE concentrations are usually shown for a given meteorite. These do not, however, necessarily reflect the maximum zoning present (or observed) in these phases. Some minor variation of the REE concentrations is also observed in anorthite from some of the angrites. REE patterns are shown in Figure 1. Below we discuss the results for each meteorite in detail.

3.1. LEW 86010

This is the second angrite to be found and initial descriptions showed that it differed substantially in mineralogy and texture

Table 2. Representative elemental concentrations in clinopyroxene.

	LEW86 (l)	LEW86 (h)	LEW87 (l)	LEW87 (h)	A88 (l)	A88 (h)	S99 (l)	S99 (h)	DOR (l)	DOR (h)
Na	26 ± 1	52 ± 1	38 ± 1	67 ± 1	38 ± 1	60 ± 2	29 ± 1	44 ± 1	32 ± 1	130 ± 2
Mg (%)	7.3 ± 0.1	4.7 ± 0.1	4.6 ± 0.1	2.3 ± 0.1	4.7 ± 0.1	2.9 ± 0.1	4.3 ± 0.1	1.2 ± 0.1	6.0 ± 0.1	0.13 ± 0.01
K	3.4 ± 0.1	5.9 ± 0.1	12 ± 1	14 ± 1	2.9 ± 0.4	6.0 ± 0.5	3.0 ± 0.2	3.1 ± 0.2	12 ± 1	38 ± 1
Ca (%)	14.7 ± 0.2	14.2 ± 0.5	15.8 ± 0.1	17.2 ± 0.1	17.0 ± 0.4	18.9 ± 0.5	15.1 ± 0.1	14.8 ± 0.1	14.7 ± 0.1	15.1 ± 0.1
Sc	192 ± 2	68 ± 5	133 ± 1	29 ± 1	204 ± 5	71 ± 5	187 ± 1	87 ± 1	219 ± 1	11 ± 1
Ti	4,445 ± 6	18,400 ± 20	7,115 ± 19	10,540 ± 25	8460 ± 54	14,420 ± 62	9,190 ± 15	14,650 ± 27	7,020 ± 14	19,920 ± 42
V	734 ± 1	233 ± 1	177 ± 1	28 ± 1	582 ± 6	121 ± 2	425 ± 2	119 ± 1	587 ± 2	15 ± 1
Cr	5,605 ± 3	1,350 ± 2	756 ± 3	118 ± 1	1820 ± 15	137 ± 3	1,150 ± 4	76 ± 1	2,295 ± 6	6.2 ± 0.5
Mn	842 ± 1	927 ± 2	1895 ± 4	2625 ± 6	1400 ± 15	1,940 ± 13	1,380 ± 5	1,720 ± 7	1,080 ± 4	1,560 ± 8
Fe (%)	6.0 ± 0.1	9.3 ± 0.1	12.7 ± 0.1	20.4 ± 0.1	10.5 ± 0.1	17.0 ± 0.1	11.5 ± 0.1	17.6 ± 0.1	9.0 ± 0.1	23.2 ± 0.1
Sr			19 ± 1	35 ± 1	23 ± 1	30 ± 1	17 ± 1	32 ± 1	12 ± 1	70 ± 1
Y	12 ± 1	63 ± 1	21 ± 1	31 ± 1	20 ± 1	31 ± 1	21 ± 1	31 ± 1	19 ± 1	64 ± 1
Zr	38 ± 1	277 ± 1	97 ± 1	179 ± 2	122 ± 5	228 ± 5	121 ± 2	199 ± 3	82 ± 1	360 ± 4
Ba	0.23 ± 0.01	0.46 ± 0.03	0.61 ± 0.09	1.7 ± 0.2	0.59 ± 0.09	0.20 ± 0.04	0.044 ± 0.012	0.18 ± 0.03	1.7 ± 0.2	8.7 ± 0.7
La	0.44 ± 0.03	4.4 ± 0.1	0.89 ± 0.06	1.6 ± 0.1	0.90 ± 0.11	1.6 ± 0.1	1.1 ± 0.1	1.9 ± 0.1	0.66 ± 0.05	4.9 ± 0.4
Ce	1.8 ± 0.1	18 ± 1	3.6 ± 0.2	6.6 ± 0.3	3.5 ± 0.4	6.7 ± 0.5	4.3 ± 0.2	8.3 ± 0.4	2.7 ± 0.2	17 ± 1
Pr	0.37 ± 0.02	3.3 ± 0.1	0.68 ± 0.05	1.2 ± 0.1	0.85 ± 0.09	1.3 ± 0.1	0.82 ± 0.05	1.5 ± 0.1	0.54 ± 0.04	3.4 ± 0.3
Nd	2.2 ± 0.1	19 ± 1	4.5 ± 0.2	6.6 ± 0.2	4.8 ± 0.3	7.1 ± 0.4	4.8 ± 0.2	8.3 ± 0.3	3.3 ± 0.1	17 ± 1
Sm	0.99 ± 0.07	6.4 ± 0.3	1.6 ± 0.1	2.6 ± 0.2	1.7 ± 0.2	2.7 ± 0.2	1.8 ± 0.2	2.8 ± 0.2	1.7 ± 0.1	5.8 ± 0.5
Eu	0.26 ± 0.01	1.5 ± 0.1	0.33 ± 0.03	0.52 ± 0.04	0.44 ± 0.05	0.60 ± 0.06	0.43 ± 0.03	0.74 ± 0.04	0.35 ± 0.03	1.5 ± 0.1
Gd	1.6 ± 0.1	8.9 ± 0.4	2.4 ± 0.2	3.5 ± 0.3	2.4 ± 0.4	4.6 ± 0.4	2.6 ± 0.2	4.0 ± 0.3	2.3 ± 0.2	5.6 ± 0.9
Tb	0.28 ± 0.02	1.5 ± 0.1	0.51 ± 0.04	0.57 ± 0.06	0.43 ± 0.1	0.88 ± 0.11	0.54 ± 0.05	0.76 ± 0.06	0.42 ± 0.04	1.1 ± 0.2
Dy	1.8 ± 0.1	9.7 ± 0.2	3.5 ± 0.2	4.8 ± 0.2	3.6 ± 0.3	5.1 ± 0.2	3.1 ± 0.1	4.7 ± 0.2	2.7 ± 0.1	8.0 ± 0.5
Ho	0.34 ± 0.02	1.9 ± 0.1	0.77 ± 0.04	1.0 ± 0.1	0.72 ± 0.07	1.1 ± 0.1	0.71 ± 0.05	1.0 ± 0.1	0.63 ± 0.05	1.7 ± 0.2
Er	0.83 ± 0.04	4.3 ± 0.1	2.1 ± 0.1	3.3 ± 0.1	2.1 ± 0.2	3.3 ± 0.2	2.0 ± 0.1	3.2 ± 0.1	1.7 ± 0.1	4.8 ± 0.3
Tm	0.099 ± 0.007	0.46 ± 0.03	0.32 ± 0.02	0.45 ± 0.04	0.27 ± 0.07	0.43 ± 0.05	0.31 ± 0.03	0.45 ± 0.04	0.23 ± 0.02	0.73 ± 0.09
Yb	b.d.	b.d.	2.3 ± 0.1	b.d.	2.0 ± 0.2	3.2 ± 0.3	1.9 ± 0.2	3.7 ± 0.3	1.8 ± 0.2	5.3 ± 0.6
Lu	b.d.	b.d.	b.d.	b.d.	0.33 ± 0.07	0.58 ± 0.08	0.34 ± 0.05	0.58 ± 0.06	0.23 ± 0.03	0.82 ± 0.13
fe#	27	46	55	79	49	72	54	86	39	99

In ppm, except as noted; b.d.: below detection; empty space: not measured; 'l' and 'h' refer to analyses with lower and higher REE concentrations, respectively.

from Angra dos Reis. It has a hypidiomorphic-granular texture with grain sizes ranging up to ~2.5 mm (Delaney and Sutton, 1988; McKay et al., 1988a). McKay et al. (1988a) note that it contains ~45% clinopyroxene with the remainder consisting of subequal amounts of plagioclase and olivine (including kirschsteinite), minor troilite and merrillite, and trace spinel. As noted earlier, although Crozaz and McKay (1990) reported trace element data for the individual minerals of LEW 86010, we made a number of additional measurements for olivine and plagioclase. The new measurements are generally consistent with the older ones, and do not significantly extend the range of trace element compositions observed in this meteorite. Except as noted, the data reported herein represent new measurements or older measurements not explicitly reported by Crozaz and McKay (1990).

Plagioclase is subhedral to euhedral and is almost pure anorthite (~An_{100}) in composition (Delaney and Sutton, 1988). Its REE pattern is LREE-enriched with a large positive Eu anomaly, as expected for this mineral (Fig. 1a). REE concentrations show some variability, particularly for the LREE (Table 1). Olivine grains (Fa_{68}) are subhedral to anhedral and contain exsolution lamellae of Fe-rich (Fa_{79}) kirschsteinite (Delaney and Sutton, 1988; Goodrich, 1988; Crozaz and McKay, 1990). Major element compositions are uniform (McKay et al., 1988a) and trace element compositions also show little variation. The REE pattern is strongly HREE-enriched with little Eu anomaly (Fig. 1a). The REE abundances in kirschsteinite are also uniform and, for the LREE, are more than a 1 order of magnitude higher than those in olivine. However, the slope of the REE pattern is much less steep than that of olivine and both phases have similar HREE abundances (Fig. 1a). Clinopyroxene occurs as anhedral grains or clusters with variable major and minor element abundances (McKay et al., 1988a). Larger grains are zoned from Mg-rich cores with fe# values (molar Fe/Fe + Mg) from 0.24 to 0.28 to rims that are enriched in Fe (fe# up to 0.48), Ti and Al (Delaney and Sutton, 1988; Goodrich, 1988). Crozaz and McKay (1990) noted that REE concentrations are correlated with fe# and vary by an order of magnitude. Figure 1a and Table 2 show the range of compositions observed. Finally, Crozaz and McKay (1990) measured five merrillite grains in LEW 86010. REE concentrations are uniform (Table 4) and the pattern is strongly LREE-enriched with a small negative Eu anomaly (Fig. 1f; see also Fig. 1 of Crozaz and McKay, 1990).

3.2. LEW 87051

With a mass of only 0.6 g, LEW 87051 is the smallest known angrite. It has a porphyritic texture with large olivine grains embedded in a fine-grained groundmass of euhedral laths of anorthite (An_{100}) intergrown with euhedral to subhedral zoned clinopyroxene and olivine (McKay et al., 1990; Prinz et al., 1990; Mittlefehldt et al., 1998). The fine-grained portion of the rock contains subequal amounts of clinopyroxene and anorthite, with lesser olivine and kirschsteinite (Prinz et al., 1990). The large olivine grains, which make up ~25 vol.% of the meteorite, are significantly more Mg-rich (Fa_{17-21} with a few grains up to Fa_9) than groundmass olivines, which range up to

Table 3. Representative elemental concentrations in olivine (including kirschsteinite).

	LEW86 (l)	LEW86 (h)	LEW87[a]	A88 (l)[a]	A88 (h)	S99 (l)	S99 (h)	DOR (l)	DOR (h)
Na	4.5 ± 0.1	78 ± 1	3.3 ± 0.1	3.1 ± 0.1	84 ± 1	6.5 ± 0.2	13 ± 1	12 ± 1	26 ± 1
Mg (%)	9.4 ± 0.1	4.7 ± 0.1	25.2 ± 0.1	24.9 ± 0.1	1.2 ± 0.1	22.0 ± 0.1	0.98 ± 0.01	22.2 ± 0.1	1.5 ± 0.1
K	3.3 ± 0.1	22 ± 1	1.9 ± 0.1	3.5 ± 0.1	19 ± 1	0.83 ± 0.10	1.3 ± 0.1	3.5 ± 0.2	6.3 ± 0.3
Ca (%)	2.8 ± 0.1	30.6 ± 0.1	0.36 ± 0.01	0.20 ± 0.01	17.8 ± 0.1	0.54 ± 0.01	7.4 ± 0.1	0.68 ± 0.01	8.7 ± 0.1
Sc	6.6 ± 0.1		9.4 ± 0.1	3.6 ± 0.1	1.3 ± 0.3	16 ± 1	4.6 ± 0.3	21 ± 1	7.2 ± 0.3
Ti	293 ± 1	587 ± 3	65 ± 1	58 ± 1	682 ± 3	104 ± 2	637 ± 3	135 ± 1	807 ± 4
V	3.8 ± 0.1	1.1 ± 0.1	46 ± 1	29 ± 1	0.23 ± 0.02	26 ± 1	0.95 ± 0.07	35 ± 1	2.0 ± 0.1
Cr	105 ± 1	51 ± 1	1,090 ± 2	2,030 ± 4	11 ± 1	419 ± 3	9.2 ± 0.3	463 ± 2	16 ± 1
Mn	6,945 ± 5	5,740 ± 6	1,960 ± 3	841 ± 2	8,195 ± 12	3,245 ± 8	9,890 ± 18	3,470 ± 6	9,750 ± 17
Fe (%)	43.9 ± 0.1	32.2 ± 0.1	13.0 ± 0.1	4.9 ± 0.1	45.4 ± 0.1	22.9 ± 0.1	60.1 ± 0.1	28.3 ± 0.1	64.4 ± 0.1
Sr	0.57 ± 0.03		0.042 ± 0.007	0.13 ± 0.02	10 ± 1	0.083 ± 0.020	1.6 ± 0.1	0.21 ± 0.03	1.5 ± 0.1
Y	15 ± 1	51 ± 1	0.27 ± 0.02	0.17 ± 0.01	18 ± 1	0.41 ± 0.03	8.4 ± 0.3	0.34 ± 0.02	8.0 ± 0.3
Zr	0.32 ± 0.02	0.22 ± 0.02	0.11 ± 0.02	0.12 ± 0.01	0.61 ± 0.04	0.10 ± 0.02	0.68 ± 0.04	0.36 ± 0.04	1.2 ± 0.1
Ba	0.11 ± 0.01	0.86 ± 0.07	0.075 ± 0.014	0.035 ± 0.008	0.37 ± 0.03	0.12 ± 0.03	0.15 ± 0.02	1.4 ± 0.1	2.7 ± 0.2
La	0.013 ± 0.001	0.37 ± 0.03	b.d.	b.d.	0.070 ± 0.006	b.d.	0.026 ± 0.005	b.d.	b.d.
Ce	0.069 ± 0.005	1.6 ± 0.1	b.d.	b.d.	0.33 ± 0.02	b.d.	0.12 ± 0.02	b.d.	b.d.
Pr	0.014 ± 0.001	0.39 ± 0.03	b.d.	b.d.	0.075 ± 0.008	b.d.	0.018 ± 0.004	b.d.	b.d.
Nd	0.13 ± 0.01	2.0 ± 0.1	b.d.	b.d.	0.53 ± 0.02	b.d.	0.15 ± 0.02	0.0032 ± 0.0027	0.12 ± 0.01
Sm	0.092 ± 0.008	1.3 ± 0.1	b.d.	b.d.	0.30 ± 0.02	b.d.	0.058 ± 0.018	0.0018 ± 0.0032	0.060 ± 0.014
Eu	0.035 ± 0.002	0.36 ± 0.02	0.0006 ± 0.0005	b.d.	0.11 ± 0.01	b.d.	0.032 ± 0.005	b.d.	0.039 ± 0.008
Gd	0.36 ± 0.01	1.8 ± 0.2	0.0044 ± 0.0022	0.0080 ± 0.002	0.71 ± 0.05	0.0046 ± 0.0038	0.20 ± 0.03	b.d.	0.23 ± 0.03
Tb	0.13 ± 0.01	0.54 ± 0.04	0.0029 ± 0.0009	0.0020 ± 0.001	0.19 ± 0.01	0.0043 ± 0.0025	0.088 ± 0.013	b.d.	0.058 ± 0.008
Dy	1.4 ± 0.1	4.7 ± 0.2	0.027 ± 0.003	0.020 ± 0.003	1.9 ± 0.1	0.019 ± 0.006	0.78 ± 0.04	0.031 ± 0.006	0.72 ± 0.04
Ho	0.44 ± 0.02	0.90 ± 0.1	0.0064 ± 0.0012	0.0039 ± 0.0013	0.49 ± 0.03	0.0078 ± 0.0032	0.19 ± 0.02	0.0082 ± 0.0024	0.27 ± 0.02
Er	1.8 ± 0.1	2.6 ± 0.1	0.045 ± 0.004	0.020 ± 0.003	1.8 ± 0.1	0.043 ± 0.008	1.0 ± 0.1	0.040 ± 0.006	0.95 ± 0.05
Tm	0.32 ± 0.02	0.31 ± 0.02	0.0082 ± 0.0014	0.0037 ± 0.0013	0.30 ± 0.02	0.0036 ± 0.0025	0.21 ± 0.02	0.015 ± 0.003	0.16 ± 0.02
Yb	2.5 ± 0.1	b.d.	0.070 ± 0.007	0.029 ± 0.008	2.3 ± 0.1	0.082 ± 0.022	1.5 ± 0.1	0.086 ± 0.017	1.4 ± 0.1
Lu	0.44 ± 0.02	b.d.	0.013 ± 0.002	0.0083 ± 0.0022	0.33 ± 0.03	0.016 ± 0.005	0.24 ± 0.02	0.018 ± 0.005	0.22 ± 0.02
fe#	67	75	18	8	94	31	96	36	95

In ppm, except as noted; b.d.: below detection; empty space: not measured; 'l' and 'h' refer to analyses with lower and higher REE concentrations, respectively.
[a] Megacryst core.

virtually Mg-free compositions (McKay et al., 1990), and have been interpreted to be xenocrysts (Prinz et al., 1990; Mikouchi et al., 1996). Due to the very limited amount of material available, we were only able to obtain one good full REE analysis each for plagioclase and olivine. The plagioclase pattern is shown in Figure 1b. The olivine we measured is the core of a large megacryst. It has a HREE-enriched pattern (Fig. 1b) with low REE abundances (Table 3); only REE heavier than Sm are above detection limits. Clinopyroxene in LEW 87051 shows strong zonation of the major elements (fe# from ~0.4 to >0.99) from the cores to the rims of grains (McKay et al., 1990; Prinz et al., 1990; Mittlefehldt et al., 1998). However, we observe REE zoning of less than a factor of 2 (Figure 1b, Table 2). The true extent of zoning is probably larger than this, as it was not possible to analyze the most Fe-rich zones of the clinopyroxenes, due to the fine grain size of this meteorite (McKay et al., 1990). A single merrillite grain has very high REE abundances (Table 4) but a REE pattern that is less steep than that of LEW 86010 (Fig. 1f).

Table 4. REE concentrations in phosphate.

	LEW86[a]	LEW87	S99
La	816 ± 55	1085 ± 25	780 ± 61
Ce	1575 ± 78	2720 ± 45	2175 ± 25
Pr	164 ± 6	342 ± 13	275 ± 15
Nd	705 ± 20	1845 ± 41	1165 ± 95
Sm	148 ± 4	440 ± 30	294 ± 22
Eu	28 ± 1	115 ± 6	83 ± 3
Gd	136 ± 4	523 ± 35	334 ± 29
Tb	22 ± 1	108 ± 10	76 ± 4
Dy	115 ± 5	711 ± 26	429 ± 24
Ho	20 ± 1	146 ± 10	90 ± 1
Er	33 ± 2	390 ± 18	251 ± 16
Tm	2.7 ± 0.4	60 ± 5	33 ± 2
Yb	b.d.	305 ± 20	168 ± 5
Lu	b.d.	40 ± 5	19 ± 1

In ppm. [a] Average of five analyses, data from Crozaz and McKay (1990).

3.3. Asuka 881371

This angrite is texturally very similar to LEW 87051 (Mikouchi et al., 1996). It has a porphyritic texture consisting of olivine megacrysts set in a finer-grained ophitic groundmass of olivine, plagioclase and clinopyroxene (Yanai, 1994; Prinz and Weisberg, 1995; Mikouchi et al., 1996). However, the modal volume of these megacrysts is significantly less (5 vs. 25 vol.%) than in LEW 87051 (Warren and Davis, 1995) and the groundmass of Asuka 881371 is somewhat more coarse-grained than that of LEW 87051 (Prinz and Weisberg, 1995; Mikouchi et al., 1996). Just as for LEW 87051, Mikouchi et al. (1996) and McKay et al. (1995b) argued, on the basis of their chemistry, that the large olivine grains are xenocrystic. Core compositions are mostly Fa_{11}, but some cores are more Fe-rich

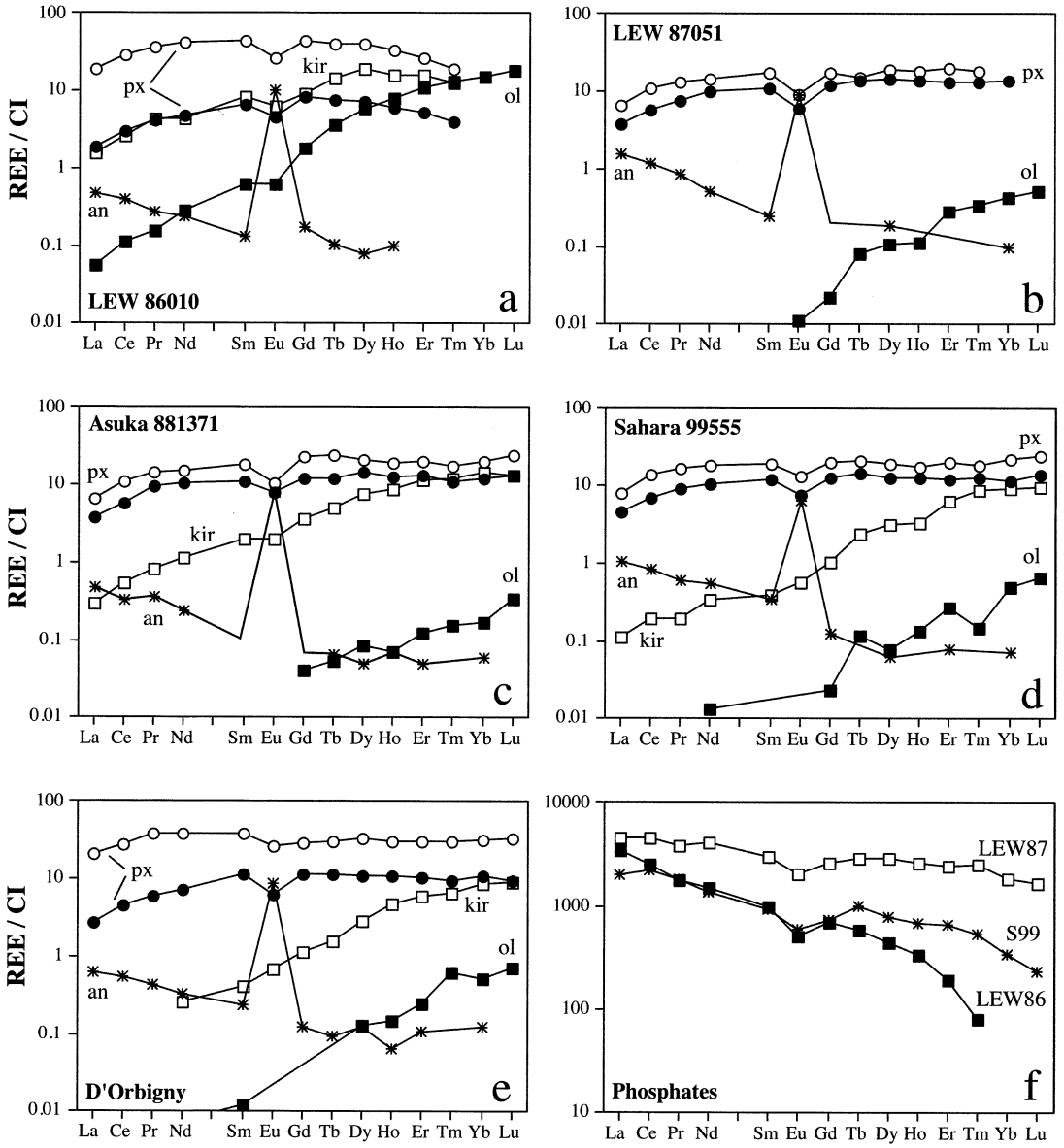

Fig. 1. Representative CI chondrite-normalized REE patterns for individual minerals from the angrites. (a) LEW 86010; (b) LEW 87051; (c) Asuka 881371; (d) Sahara 99555; (e) D'Orbigny; and (f) phosphates from LEW 86010 (LEW86), LEW 87051 (LEW87) and Sahara 99555 (S99). Note the different scale for graph (f). Abbreviations: an: anorthite; px: pyroxene; kir: kirschsteinite; ol: olivine. Data for LEW 86010 phosphate from Crozaz and McKay (1990).

(Fa_{20}). The REE pattern for one of these olivine megacrysts is shown in Figure 1c. REE abundances are somewhat lower than those of the megacryst from LEW 87051 (Table 3) and all REE lighter than Gd are below detection. Groundmass olivines are strongly zoned from cores of ~Fa_{30} to nearly Mg-free rims consisting of intergrowths of kirschsteinite and Ca-rich fayalite (Mikouchi et al., 1996). Kirschsteinite in Asuka 881371 has a REE pattern that is parallel to that of olivine, but with abundances that are 1 to 2 orders of magnitude higher (Fig. 1c). The REE in plagioclase, which as in the other angrites is nearly pure anorthite ($An_{>99.5}$), extend to somewhat lower abundances in Asuka 881371 than in the other angrites (Table 1, Fig. 1). As in LEW 87051, clinopyroxene is strongly zoned in major and minor elements (fe# from ~0.4 to >0.99; McKay et al., 1995a), whereas trace element zoning is more limited (factor of 2–3; Fig. 1c). This again probably reflects the fact that we did not sample the most Fe-rich portions of the clinopyroxene crystals.

3.4. Sahara 99555

Sahara 99555 is a fine-grained rock texturally similar to the groundmass portions of LEW 87051 and Asuka 881371 (Bischoff et al., 2000; Mikouchi et al., 2000a). However, olivine and plagioclase grains are euhedral to skeletal and show a complex intergrowth texture that has not been observed in the

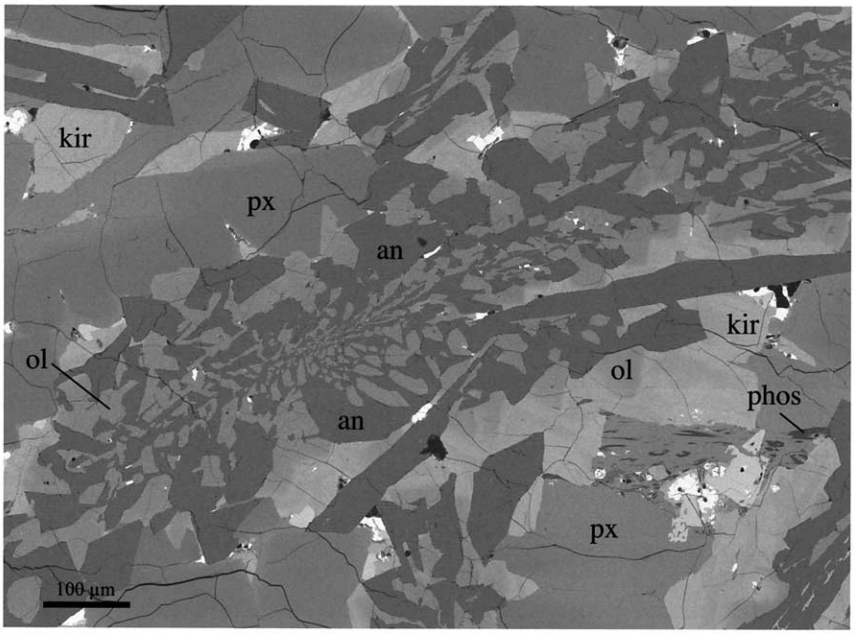

Fig. 2. Back-scattered electron (BSE) photograph of Sahara 99555, illustrating the complex intergrowth of anorthite and olivine observed in this angrite. Minor opaques (bright areas) include magnetite, spinel and troilite. Abbreviations: an: anorthite; px: pyroxene; kir: kirschsteinite; ol: olivine; phos: phosphate.

Antarctic angrites (Fig. 2). Clinopyroxene grains are subhedral to euhedral and show extensive major element zoning (fe# from ~0.5 to ~1), as in other angrites. Modal abundances of the minerals are similar to those of LEW 87051 and Asuka 881371, as are mineral compositions (olivine is zoned from Fa_{37} cores to Mg-free rims of intergrown kirschsteinite and Ca-rich fayalite, and plagioclase is essentially An_{100}), but Sahara 99555 does not appear to contain any Mg-rich olivine megacrysts (Mikouchi et al., 2000a). Olivine and kirschsteinite have parallel, HREE-enriched REE patterns (Fig. 1d) with REE abundances that are about an order of magnitude higher in kirschsteinite than in olivine. Anorthite has REE concentrations similar to that of LEW 87051 (Table 1). As in other angrites, clinopyroxene trace element zoning is correlated with core to rim zoning of the major elements. Figure 1d shows the REE patterns for the core and rim of a single grain, with REE abundances that differ by about a factor of 2. However, the maximum extent of zoning that we observed in Sahara 99555 clinopyroxene is about a factor of 4, and the true extent of zoning, as we noted for the other angrites, may be greater than this. Two grains of Ca silico-phosphate (e.g., Kaneda et al., 2001) have identical REE patterns that are similar to the pattern measured in merrillite from LEW 86010, but with less of a drop-off in the HREE (Fig. 1f).

3.5. D'Orbigny

This newest angrite is also the largest, with a mass of 16.6 kg (Mittlefehldt et al., 2002). D'Orbigny is a vesicular rock with a subophitic texture (Fig. 3) that is most similar to that of Asuka 881371 (Mikouchi and McKay, 2001). Some sections contain abundant skeletal anorthite crystals (Mittlefehldt et al., 2002) indicative of rapid crystallization, but others, including ours, do not (Mikouchi and McKay, 2001). Similarly, olivine megacrysts (Fa_{10}), like those observed in Asuka 881371 and LEW 87051, are present in some sections of D'Orbigny (Kurat et al., 2001a, 2001b; Mikouchi and McKay, 2001), but again not ours. Mikouchi and McKay (2001) estimate that D'Orbigny contains $<$ 1 vol.% of these large olivines. Unique features of D'Orbigny include its vesicular nature (Kurat et al., 2001a, 2001b; Mikouchi and McKay, 2001) and the presence of abundant glass throughout the meteorite with a major element composition similar to that of the bulk meteorite (Varela et al., 2001a, 2001b). Compositionally D'Orbigny is virtually identical to Sahara 99555 (Mittlefehldt et al., 2002) and the REE distributions we measured in D'Orbigny minerals are also very similar to those of Sahara 99555 (Fig. 1e). REE patterns in clinopyroxene show a variation of a factor of 3 to 5, similar to the maximum zoning observed in Sahara 99555. An analysis of the glass in our section shows that it has a flat REE pattern with abundances of ~10 $\times$ CI (Table 1; Fig. 4), similar to the composition of glass measured by Kurat et al. (2001c).

4. DISCUSSION

4.1. Terrestrial Weathering Effects

Terrestrial weathering is known to affect REE and other trace element abundances in meteorites from both hot and cold deserts (e.g., Crozaz et al., 2002). Although the effects are particularly problematical for whole rock data and the determination of isotopic systematics, they are also observed in the in situ measurements of individual grains. In Antarctic meteorites the chemical alteration is largely limited to the presence of Ce anomalies that can be attributed to the production of tetravalent Ce, which is less soluble than the trivalent REE,

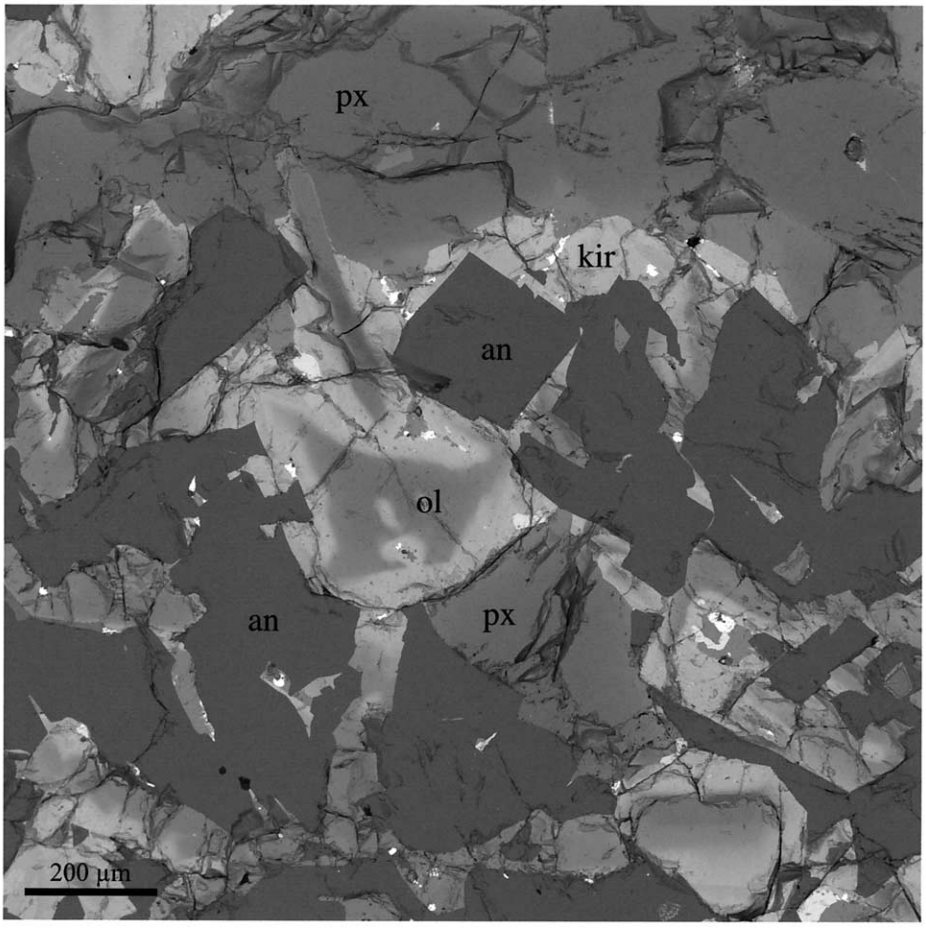

Fig. 3. Back-scattered electron (BSE) photograph of D'Orbigny, illustrating the subophitic texture of this angrite. Minor opaques (bright areas) include magnetite, spinel and troilite. Abbreviations: an: anorthite; px: pyroxene; kir: kirschsteinite; ol: olivine.

during the meteorite's exposure on the surface of the Antarctic ice (Floss and Crozaz, 1991; Mittlefehldt and Lindstrom, 1991). Cerium anomalies are also sometimes observed in hot desert meteorites, but the most common sign of terrestrial contamination is a significant enrichment of the LREE, with a typical crustal signature, often accompanied by enrichments of Sr and Ba (Crozaz and Wadhwa, 2001). Of the three Antarctic angrites studied here, we see no evidence of terrestrial alteration in any of them. However, we do observe chemical changes due to terrestrial alteration in the hot desert angrite Sahara 99555. No clinopyroxene, anorthite or phosphate grains that we analyzed are affected, but several grains of olivine and kirschsteinite exhibit LREE enrichments, together with positive Ce anomalies. Because the effects are quite pronounced and may be accompanied by other elemental changes, these analyses have been omitted from further consideration in this work. Finally, although D'Orbigny comes from neither a hot or cold desert, it was found in a farm field and initial reports note that pores contain variable amounts of caliche (Grossman and Zipfel, 2001), indicating that it probably spent an extended period on Earth before discovery. We found that several grains of olivine and kirschsteinite exhibit slight enrichments of the LREE La to Pr and have small negative Ce anomalies. The changes are subtle and appear to be limited to these elements so the data for these grains are reported here, albeit without the values for the affected elements.

4.2. REE Inventory in Angrites

To assess how well we have surveyed the REE distributions in the angrites, we compared whole rock REE compositions from the literature (Mittlefehldt and Lindstrom, 1990; Warren et al., 1995; Mittlefehldt et al., 2002) with bulk compositions calculated from our individual mineral analyses. Modal data are provided by the following sources: LEW 86010: McKay et al. (1988a); LEW 87051: McKay et al. (1990); Asuka 881371: Yanai (1994); Sahara 99555: Mikouchi et al. (2000a); D'Orbigny: Mikouchi and McKay (2001). Modal abundances of phosphate, the dominant REE carrier in the angrites, are explicitly provided only for LEW 87051 and D'Orbigny. We have, therefore, adjusted the proportion of phosphate to provide the best fit to the whole rock compositions. These amounts range from 0.2 to 0.4 vol.%, in good agreement with the estimates given by McKay et al. (1990) and Mikouchi and McKay (2001) for LEW 87051 (0.3 vol.%) and D'Orbigny (0.5 vol.%). The REE concentrations used in the calculations are

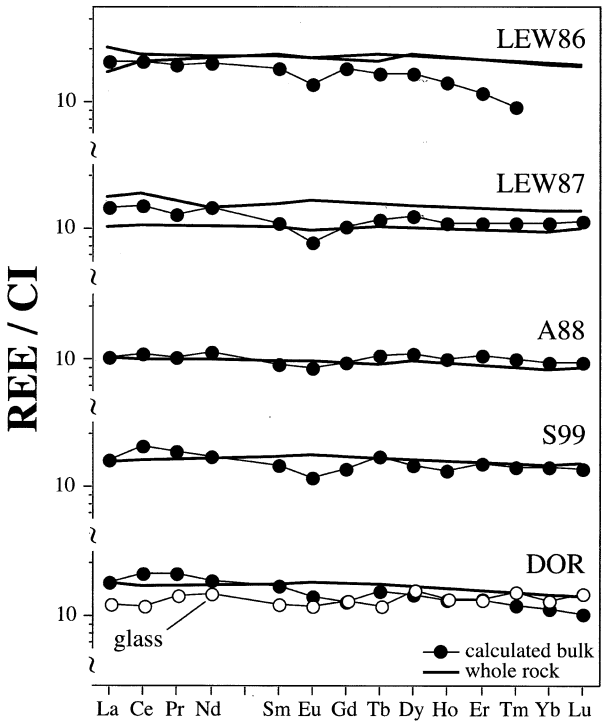

Fig. 4. CI chondrite-normalized REE patterns for angrites. Shown are whole rock REE compositions from the literature (solid lines) compared with bulk compositions calculated from the mineral data in Tables 1 to 4 (filled circles). See text for details. Also shown is the REE pattern measured for glass from D'Orbigny (open circles). Literature data for LEW86 and LEW87: Mittlefehldt and Lindstrom (1990); A88: Warren et al. (1995); S99 and DOR: Mittlefehldt et al. (2002).

listed in Tables 1 to 4. For olivine and kirschsteinite, we used the low and high REE abundances, respectively. For LEW 87051 kirschsteinite, we used the data for Asuka 881371 kirschsteinite (Table 3). For clinopyroxene we used an average of the low and high analyses for each angrite (Table 2) and for anorthite we used either an average or the single analysis given (Table 1). The phosphate REE concentrations are listed in Table 4. For Asuka 881371 and D'Orbigny we used the REE abundances of phosphate from LEW 87051 and Sahara 99555, respectively.

The results of the calculations are shown in Figure 4, where they are compared to measured whole rock REE compositions. Agreement between the calculated and measured abundances is quite good for most angrites, indicating that we have adequately measured the range of REE compositions in the minerals of these rocks. Some of the calculated whole rock compositions seem to be slightly depleted in Eu, but it is not clear that the effect is significant outside of errors. For D'Orbigny we also show the REE pattern of the glass found in this angrite. Its composition is similar to that of both the calculated and measured bulk compositions, as Kurat et al. (2001c) also noted. Two whole rock REE patterns shown for LEW 87051 differ by ~50%, while our calculated composition (modeled using 0.25 vol.% phosphate) falls between them. Varying the phosphate content from 0.2 to 0.3 vol.% accounts for the observed difference between the two measured compositions, indicating that heterogeneous distribution of phosphates is most likely responsible for the difference in the bulk analyses. The greatest discrepancy between our calculated compositions and measured whole rock abundances is for LEW 86010. Although LREE abundances agree well, our calculated abundances fall off significantly in the HREE compared to the measured values. This is largely due to the steep slope of the merrillite REE pattern (Fig. 1f). If the calculation is carried out using the REE concentrations for LEW 87051 phosphate, the calculated bulk composition is in good agreement with the measured LEW 86010 whole rock REE patterns. One possibility for the discrepancy is that the phosphates analyzed in LEW 86010 are not representative of the meteorite as a whole. Although five different grains were measured with virtually identical REE concentrations, all of them are in close spatial association within a small portion of the thin section (Crozaz and McKay, 1990). Another, more likely, explanation come from an observation by McKay et al. (1994). These authors attribute a discrepancy in the HREE between an equilibrium melt calculated from a pyroxene core (measured by Crozaz and McKay, 1990) and the bulk rock REE pattern of LEW 86010 to an inadequate mass calibration during the pyroxene analyses that led to an underestimate of the abundances of the REE heavier than Dy. Since the merrillite data were acquired at the same time as these pyroxene analyses, a similar problem probably accounts for the steep slope of the merrillite REE pattern and the resultant discrepancy between calculated and measured whole rock compositions.

4.3. Trace Element Trends in the Angrites

Crozaz and McKay (1990) showed that trace element abundances in clinopyroxene from LEW 86010 were correlated with fe#, in a manner consistent with closed system, or near closed system, crystallization. They concluded, furthermore, that Angra dos Reis and LEW 86010, despite common characteristics, must have formed in separate magmatic events. Petrographic observations, as well as experimental investigations, give clear evidence of an igneous origin for the other angrites as well. All have basaltic textures indicative of rapid crystallization (McKay et al., 1990; Mikouchi et al., 1996; Mikouchi et al., 2000a; Mikouchi and McKay, 2001). Furthermore, crystallization experiments using a synthetic Asuka 881371 groundmass analog composition (Mikouchi et al., 2000a, 2000b) and cooling rate calculations based on olivine megacryst zoning profiles (Mikouchi et al., 2001) indicate that these samples were quenched at rates corresponding to burial depths of $<$ 1 m. Below we examine the trace element trends in clinopyroxene and olivine from these angrites and compare them with those of LEW 86010.

4.3.1. Clinopyroxene

Pyroxene in the angrites is extensively zoned with fe# values increasing from the cores to the rims of crystals (Mikouchi et al., 2000a; Mikouchi and McKay, 2001; Mittlefehldt et al., 2002). We noted above that REE abundances in clinopyroxene increase from core to rim with increasing fe#. These trends are accompanied by variations in a number of other trace and minor elements. Figure 5 shows the variations in Ti, Ce, Zr, Y, V and Sc in clinopyroxene as a function of fe#. Abundances of the incompatible elements Ti, Ce, Zr and Y increase in all five angrites with increasing fe#, whereas V and Sc abundances

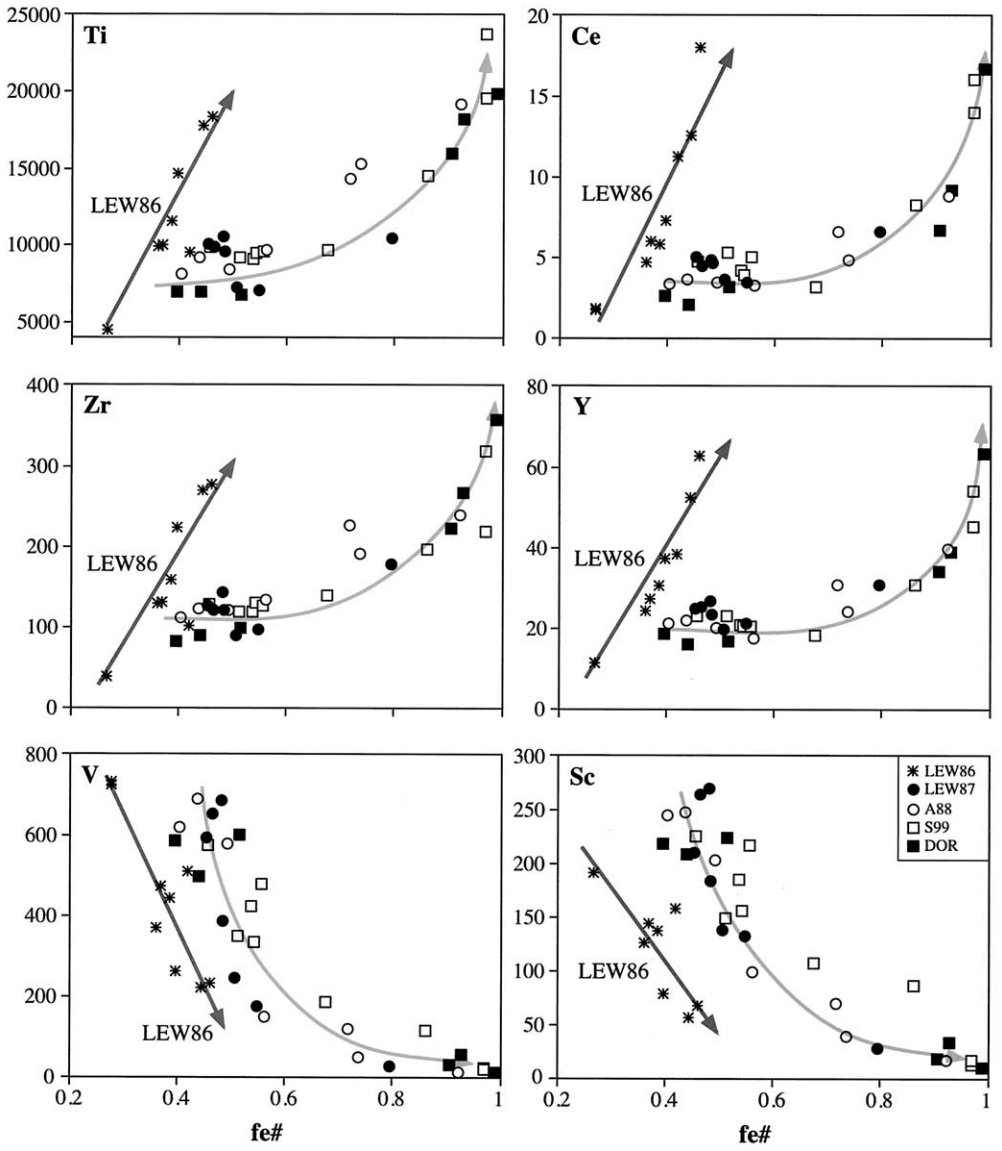

Fig. 5. Scatter plots of trace and minor element (Ti, Ce, Zr, Y, V and Sc) concentrations (in ppm) as a function of fe# in clinopyroxene from the angrites. Light grey arrows illustrate the trends observed in the angrites LEW 87051, Asuka 881371, Sahara 99555 and D'Orbigny, whereas the dark grey arrows illustrate the distinct trends for LEW 86010.

decrease. However, two distinct trends are evident, as illustrated by the arrows in Figure 5. Incompatible trace element abundances in LEW 87051, Asuka 881371, Sahara 99555 and D'Orbigny lie on a common trend, with concentrations increasing slowly at low fe# values, followed by a steep increase in the most Fe-rich clinopyroxene rims. This type of variation is consistent with the expected change in abundances of incompatible elements during closed or near-closed system crystallization under conditions rapid enough to preserve significant core to rim zoning. Scandium and V abundances decrease with increasing fe#, consistent with their expected partition coefficients indicating compatible behavior in pyroxene (e.g., Gallahan and Nielsen, 1992; Jones, 1995). Again, the data for LEW 87051, Asuka 881371, Sahara 99555 and D'Orbigny fall on a common trend.

Although the overall ranges of incompatible trace element abundances in LEW 86010 are similar to those of the other angrites (e.g., $\sim 6\times$ for Y, $\sim 8\times$ for Ce) the trend is much steeper, with the entire variation occurring over a change of fe# from ~ 0.25 to ~ 0.45. The highest incompatible trace element concentrations in LEW 86010 clinopyroxene occur at fe# values similar to those of the cores of clinopyroxene crystals from the other angrites. Scandium and V abundances in LEW 86010 clinopyroxene also decrease steeply with increasing fe#, but the trends are distinctly offset from those of the other angrites (Fig. 5).

4.3.2. Olivine

Trace and minor element variations are also evident in olivine/kirschsteinite from the angrites. Figure 6 shows the

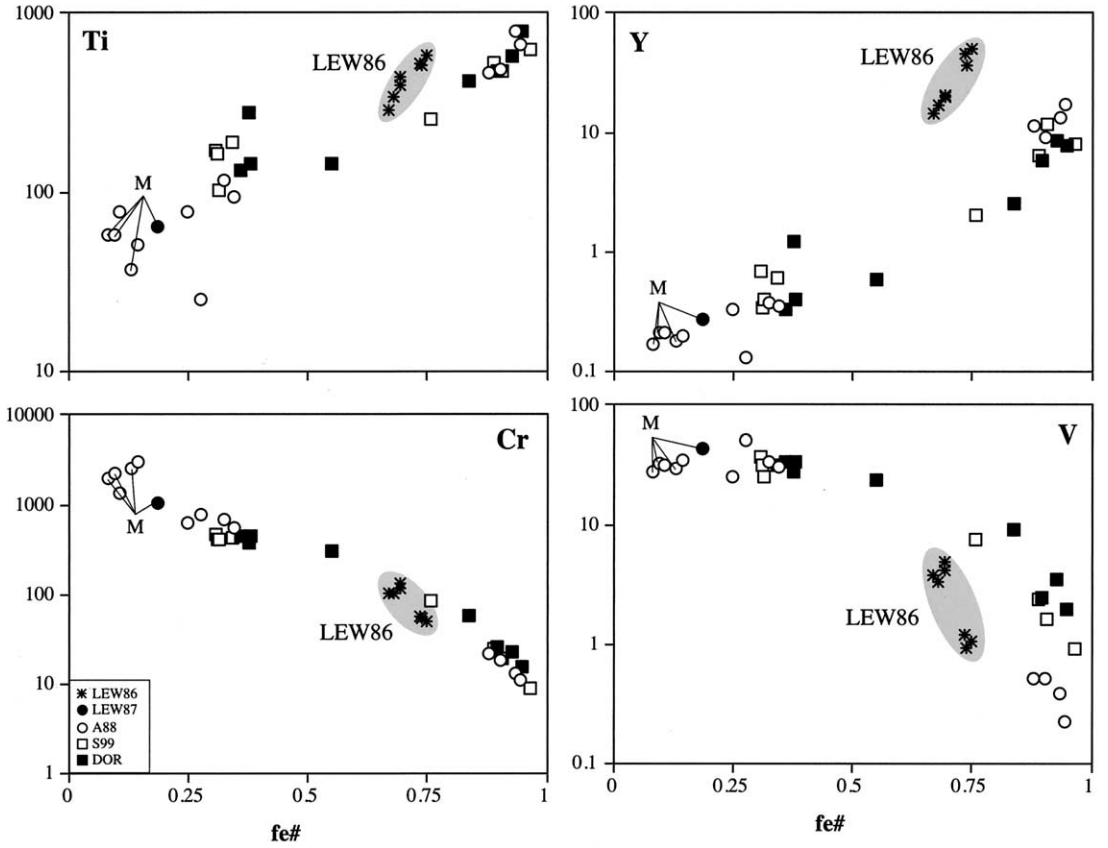

Fig. 6. Scatter plots of trace and minor element (Ti, Y, Cr and V) concentrations (in ppm) as a function of fe# in olivine/kirschsteinite from the angrites. Light grey shaded areas highlight the concentration ranges for LEW 86010. Four olivine megacrysts analyzed from LEW 87051 and Asuka 881371 are labeled with 'M'.

changes in concentrations of Ti, Y, Cr and V as a function of fe#. As for clinopyroxene, olivine compositions for the angrites LEW 87051, Asuka 881371, Sahara 99555 and D'Orbigny lie on a common trend, with abundances of the incompatible elements Ti and Y increasing with fe#, whereas the abundances of Cr and V decrease. The range of concentrations varies by 1 to 2 orders of magnitude, again consistent with crystallization under essentially closed system conditions.

The analyses from LEW 86010 show a much more limited range of compositions than the other angrites (Fig. 6), despite the fact that care was taken to analyze either pure olivine or pure kirschsteinite (Crozaz and McKay, 1990). LEW 86010 olivines have homogeneous major element compositions (Delaney and Sutton, 1988; Goodrich, 1988; McKay et al., 1988a) and, thus, the trace elements probably equilibrated to a large extent as well. Notable, furthermore, is the fact that the olivines from LEW 86010 are much more Fe-rich than the clinopyroxenes (Tables 2 and 3; Figs. 5 and 6), although this is not the case for the other angrites. McKay et al. (1988b) suggested that this may reflect equilibration of the LEW 86010 olivines with the outer Fe-rich portions of the clinopyroxenes, either during crystallization from the evolving interstitial melt, or during postcrystallization subsolidus exchange. The olivine trace element data for LEW 86010 are not as distinctly separate from that of the other angrites as is the case for clinopyroxene. Chromium abundances in LEW 86010 olivines fall along the same trend as the other angrites, and Ti and V abundances exhibit only moderate offsets from the trends. However, Y abundances are higher by an order of magnitude than those of the other angrites at similar fe# values (Fig. 6).

4.3.3. Olivine Megacrysts

Mikouchi et al. (1996) argued, on the basis of their chemistries, that the large megacrysts of olivine found in LEW 87051 and Asuka 881371 are xenocrysts that were incorporated into the magma from which the groundmass of these angrites crystallized. We analyzed the cores of four megacrysts, three from Asuka 881371 and one from LEW 87051. The grains, labeled in Figure 6, are characterized by very low fe# values and elevated Cr (>1000 ppm), as also noted by Mikouchi et al. (1996). The megacryst from LEW 87051 is more Fe-rich than those from Asuka 881371. However, this may be an artifact of the analysis (e.g., not analyzing the exact core of the crystal), as Mikouchi et al. (1996) noted that the LEW 87051 olivine cores have fe# values similar to the most Mg-rich Asuka 881371 cores. Two other olivine analyses from Asuka 881371 are compositionally similar to the megacrysts cores. These may be the type B olivines of Mikouchi et al. (1996), which are intermediate in size between the megacrysts and groundmass olivines. These authors suggested that type B olivines are also

Table 5. Equilibrium liquid compositions for angrites.

	La	Ce	Nd	Sm	Eu	Gd	Yb
$D_{fas/melt}$ [a]	0.082 ± 0.018	0.140 ± 0.030	0.304 ± 0.022	0.430 ± 0.032	0.336 ± 0.086	0.514 ± 0.067	0.447 ± 0.032
$D_{plag/melt}$ [a]	0.022	0.016	0.014	0.012 ± 0.004	0.367 ± 0.049	0.008 ± 0.003	0.004
$D_{ol/melt}$ [b]				0.00058 ± 0.00007		0.00102 ± 0.00008	0.0194 ± 0.0003
Apparent $D_{fas/melt}$	0.18–0.37	0.26–0.54	0.46–0.97	0.74–1.2	0.48–0.89	0.88–1.3	0.93–1.3
Apparent $D_{plag/melt}$	0.029–0.147	0.018–0.108	0.014–0.046	0.015–0.025	0.53–1.0	0.009–0.010	0.005–0.011
Melt compositions[c]							
LEW87 fassaite	46 ± 11	42 ± 9	33 ± 3	25 ± 3	18 ± 5	24 ± 4	31 ± 3
LEW87 anorthite	69 ± 25	73 ± 26	35 ± 12	20 ± 26	24 ± 4		24 ± 38
LEW87 (mega) olivine						22 ± 11	22 ± 2
A88 fassaite	47 ± 12	42 ± 10	35 ± 3	26 ± 4	23 ± 7	23 ± 5	28 ± 4
A88 anorthite	21 ± 7	20 ± 7	16 ± 5		21 ± 3		14 ± 12
A88 olivine							16 ± 4
A88 (mega) olivine							9 ± 1
S99 fassaite	55 ± 12	51 ± 11	35 ± 3	28 ± 3	23 ± 6	25 ± 4	27 ± 4
S99 anorthite	45 ± 15	50 ± 16	37 ± 11	27 ± 16	17 ± 3	15 ± 13	17 ± 25
S99 olivine						23 ± 19	26 ± 7
DOR fassaite	34 ± 8	32 ± 7	24 ± 2	27 ± 2	19 ± 5	23 ± 4	24 ± 3
DOR anorthite	28 ± 9	33 ± 11	23 ± 7	19 ± 8	23 ± 3	15 ± 8	29 ± 15
DOR olivine						21 ± 38	27 ± 5

[a] Data from McKay et al. (1994). [b] Data from McKay (1986). [c] CI-normalized abundances. Errors are 1σ; see text for calculation details.

xenocrysts, with smaller cores due to off-center cutting during thin sectioning.

In addition to low fe# values and elevated Cr concentrations, the megacrysts analyzed here have high V concentrations and Ti and Y abundances that fall at the low end of the range observed for all angrite olivines (Fig. 6). However, the abundances of all these elements in the megacrysts fall on extensions of the same trends observed for other olivine grains from the angrites. Thus, there appears to be some type of genetic relationship between the megacrysts and the groundmass of these angrites. They may be related to the precursor rocks from which the angrite magmas originated, and were incorporated during rapid ascent and eruption of the magmas on their parent body (e.g., Mittlefehldt et al., 2002) or added during an external heating event such as impact melting (e.g., Mikouchi et al., 1996).

4.3.4. Crystallization Trends

The trace element variations observed for clinopyroxene from the angrites LEW 87051, Asuka 881371, Sahara 99555 and D'Orbigny (Fig. 5) and the large extent of REE zonation in clinopyroxene crystals (Fig. 1) are consistent with rapid crystallization under essentially closed system conditions. Furthermore, these angrites all lie on a common trend, indicating that they crystallized from the same or very similar magmas. Trace element abundances in olivine from these angrites also lie on a common trend and show large trace element variations with fe# (Fig. 6). In contrast, although the data for LEW 86010 are also consistent with the crystallization of this angrite from a melt (e.g., Crozaz and McKay, 1990), the source magma for LEW 86010 does not appear to be the same as that for the other angrites. Trace element trends in LEW 86010 clinopyroxene are clearly distinct from those in the other angrites (Fig. 5) and LEW 86010 olivine is also compositionally different (Fig. 6).

4.4. Parent Melt Compositions

McKay et al. (1994) determined mineral/melt partition coefficients for clinopyroxene and anorthite using a synthetic LEW 86010 bulk composition and conditions appropriate for angrite formation. Using these *D* values and REE concentrations from the cores of clinopyroxene and anorthite crystals (i.e., the lowest concentrations observed, Tables 1–2), we can calculate the REE compositions of the melts in equilibrium with these minerals for each of the angrites. McKay et al. (1994) found a bimodal distribution of Al contents in their pyroxene analyses (4–7 vs. 8–11 wt.%) and observed that the REE partition coefficients for clinopyroxene vary with the Al. These authors noted that the pyroxene cores of LEW 86010 have Al_2O_3 contents similar to the average of their experimental pyroxene analyses with Al contents of < 7.0 wt.%, and, therefore, used only these analyses to determine partition coefficients for calculating melts in equilibrium with LEW 86010 clinopyroxene. Clinopyroxene cores from the other angrites studied here have Al_2O_3 contents ranging from ~7 to 9 wt.% (McKay et al., 1990; Mikouchi et al., 1996; Bischoff et al., 2000; Mikouchi and McKay, 2001; Mittlefehldt et al., 2002). Therefore, to calculate the compositions of melts in equilibrium with clinopyroxene from these angrites, we used the partition coefficients determined from all the pyroxene analyses of McKay et al. (1994). These are listed in Table 5 and have an average Al_2O_3 content of 7.5 wt.%.

The results of our calculations are presented in Table 5 and are shown graphically in Figure 7, where they are compared to the bulk composition of each meteorite. Results are not shown for LEW 86010 because our calculations for this meteorite are essentially identical to those of McKay et al. (1994), who found that the liquids calculated from clinopyroxene and anorthite cores are in excellent agreement with each other, indicating that both minerals crystallized in equilibrium from the same melt (see their Fig. 3). Moreover, the equilibrium melts agree well with the bulk composition of LEW 86010, indicating that

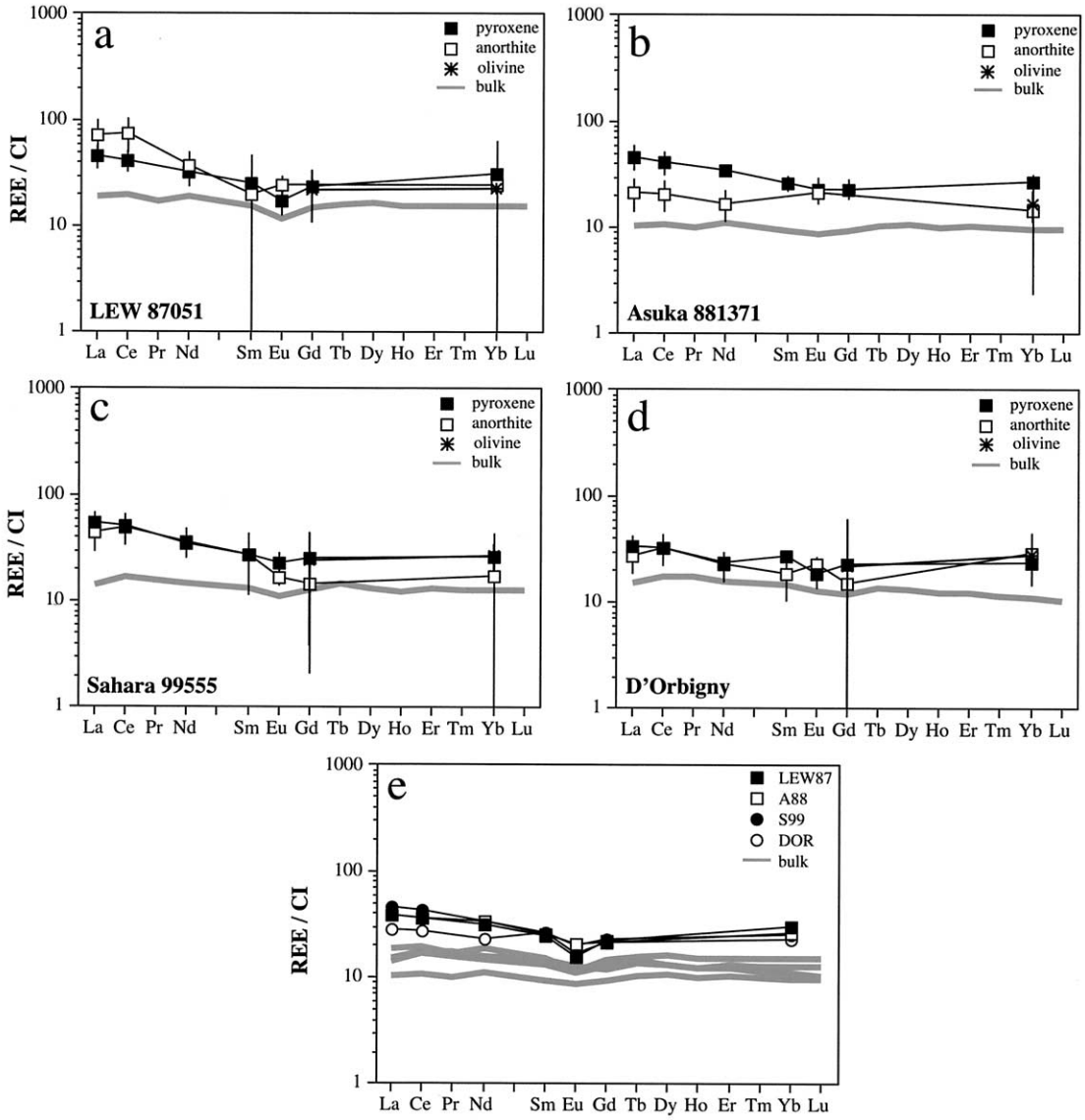

Fig. 7. CI chondrite-normalized REE patterns for calculated melts in equilibrium with anorthite (open squares), clinopyroxene (filled squares) and olivine (asterisks) compared with the bulk REE pattern (gray line) for each angrite. (a) LEW 87051; (b) Asuka 881371; (c) Sahara 99555; (d) D'Orbigny; (e) calculated pyroxene melts compared with bulk REE patterns. For LEW 87051 and Asuka 881371, the bulk compositions are for the groundmass portions only of these meteorites.

crystallization proceeded under essentially closed system conditions. The liquids calculated to be in equilibrium with clinopyroxene and anorthite from the other angrites have flat to somewhat LREE-enriched patterns and abundances that range from ~10 to 50 × CI (Table 5; Fig. 7). For LEW 87051, Sahara 99555 and D'Orbigny, the compositions of the liquids calculated from these two minerals are in excellent agreement with each other, indicating that anorthite and clinopyroxene crystallized in equilibrium from the same melt. The melt in equilibrium with anorthite from Asuka 881371 has LREE abundances that are somewhat lower than the melt in equilibrium with clinopyroxene.

Although no partition coefficients are available for olivine using angrite compositions, *D* values were determined by McKay (1986) for olivine/melt REE partitioning using synthetic lunar compositions. These experiments were also carried out under somewhat more reducing conditions (IW + 0.5) than those appropriate for angrite formation. Nevertheless, we find that the liquids calculated from core olivines of Sahara 99555 and D'Orbigny, using these *D* values, have Gd and Yb abundances of 21 to 27 × CI, in excellent agreement with those of clinopyroxene and anorthite from these angrites (Table 5). Both LEW 87051 and Asuka 881371 contain olivine megacrysts, which appear to have a distinct origin, and groundmass olivine thought to have crystallized together with anorthite and clinopyroxene. Melt in equilibrium with groundmass olivine from Asuka 881371 has Yb abundances that agree, within errors, with those of parent melts for clinopyroxene and anorthite from

this angrite (Table 5, Fig. 7). The melt in equilibrium with megacrystic olivine from Asuka 881371 has a Yb abundance of 10 × CI, somewhat lower than the REE abundances of the parent melt calculated for anorthite and 3 times lower than the melt in equilibrium with clinopyroxene (Table 5). This again emphasizes the distinctiveness of these megacrystic grains. Only one olivine, a megacrystic grain, was analyzed in LEW 87051. The melt in equilibrium with this grain has REE abundances similar to those of the melts calculated from clinopyroxene and anorthite (Fig. 7, Table 5), despite the fact megacrystic olivine from Asuka 881371 has a lower parent melt REE composition. As we noted earlier, this may be an artifact of the analysis (e.g., not analyzing the exact core of the grain), as this olivine is more Fe-rich than the megacrysts from Asuka 881371. Finally, we note that melt compositions calculated for clinopyroxene from all four angrites are identical within errors (Fig. 7e, Table 5), providing strong evidence that these meteorites all crystallized from very similar, if not the same, magmas. These results are consistent with the trace elements trends discussed in the previous section.

Experimental and petrographic studies indicate a crystallization sequence of olivine, then plagioclase and finally pyroxene for the angrites (McKay et al., 1991; Longhi, 1999; Mittlefehldt et al., 2002), although textural evidence suggests that all three phases crystallized simultaneously for much of the sequence (e.g., Mikouchi et al., 1996; Mittlefehldt et al., 2002). Our data are also consistent with essentially simultaneous crystallization of the major phases, including olivine. However, the anorthite and olivine parent melt compositions for Asuka 881371 have somewhat lower REE abundances than its clinopyroxene parent melt composition; this may provide evidence that some olivine and plagioclase crystallization preceded that of clinopyroxene in this angrite.

As noted earlier, the large variations in trace element abundances observed in clinopyroxene and olivine/kirschsteinite (Figs. 5 and 6) indicate crystallization under essentially closed system conditions, implying that these angrites represent melt compositions. Figure 7 also compares the compositions of the melts in equilibrium with anorthite and clinopyroxene with the bulk REE compositions determined for the angrites. For LEW 87051 and Asuka 881371, the bulk REE compositions shown in Figure 7 represent only the groundmass portions of these meteorites. Bulk REE abundances for each of the four angrites are 2 to 5 times lower than the REE abundances of the melts calculated to be in equilibrium with their respective core clinopyroxenes (Fig. 7e). Furthermore, except for D'Orbigny, the melt compositions tend to be LREE-enriched relative to the meteorite bulk compositions (Fig. 7). McKay et al. (1990, 1995a) noted that the most Mg-rich pyroxenes in both LEW 87051 and Asuka 881371 are too Fe-rich to have crystallized from the calculated melt compositions and argue that pyroxene crystallization can only have begun after crystallization of large amounts of olivine from the initial melt. The elevated REE abundances (relative to bulk compositions) and LREE-rich compositions of the calculated pyroxene parent melts would be consistent with this scenario. However, although we noted above that there is some indication that some olivine may have crystallized before pyroxene in Asuka 881371, this appears to have been accompanied by anorthite crystallization, which would not lead to the required LREE enrichment in the fassaite parent melt. Moreover, in general the trace element data do not provide compelling support for crystallization of significant amounts of olivine before pyroxene in most of the angrites.

Because textures in the angrites indicate that they have experienced very rapid cooling, another possibility to consider is whether or not kinetic effects may be affecting the calculated melt compositions. Kennedy et al. (1993) carried out an experimental study of trace element partitioning in chondrules and evaluated the role that rapid cooling has on partition coefficients. They found that for both olivine and orthopyroxene, apparent partition coefficients for incompatible trace elements are up to three orders of magnitude greater than equilibrium values. Furthermore, both Kennedy et al. (1993) and Jones and Layne (1997), who carried out a similar study, found that LREE/HREE ratios of apparent partition coefficients increase at high cooling rates.

We can calculate apparent D values for clinopyroxene and anorthite in the angrites using their core REE concentrations and assuming that they crystallized from melts with the REE abundances of their bulk compositions. The apparent partition coefficients thus determined for clinopyroxene are shown in Table 5 and are between 1.5 and 4.5 times higher than the D values of McKay et al. (1994). In addition, the LREE/HREE ratios of the apparent values are somewhat elevated, although the difference is not large (a factor of < 2). We see similar effects in the apparent D values calculated for anorthite, but since plagioclase was not investigated in either of the experimental studies, it is difficult to evaluate whether kinetic effects are responsible. In particular, it is not clear if rapid cooling would result in higher LREE/HREE ratios in plagioclase as it appears to do in pyroxene and olivine. The cooling rates investigated by Kennedy et al. (1993) are far higher (1000–2000°C/h) than estimates of the cooling rates for the angrites (≤50°C/h; Mikouchi et al., 2001), but the effects that we observe on apparent partition coefficients are also significantly smaller than those seen by Kennedy et al. (1993). These results suggest that kinetic effects due to the rapid crystallization of the angrites probably resulted in non-equilibrium partitioning of the REE. This may be responsible, in large part, for the discrepancy between bulk REE compositions and melts calculated to be in equilibrium with the major crystallizing phases.

4.5. Crystallization Histories

We noted above that the trace element data strongly support a common origin for the four angrites LEW 87501, Asuka 881371, Sahara 99555 and D'Orbigny, while indicating a separate origin for LEW 86010. Mittlefehldt et al. (2002) argued that major element bulk compositional data suggest complex origins for the angrites and noted that "no simple petrogenetic sequence, partial melting with or without fractional crystallization can explain the angrite suite." Moreover, they suggested that D'Orbigny experienced local additions of more primitive melt during its crystallization. The angrites do indeed show some differences in major element compositions (e.g., fe#, Fe/Mn ratios), even after normalization to account for the presence of olivine xenocrysts in LEW 87051 and Asuka 881371. However, Mittlefehldt et al. (2002) also noted that all the angrites (except Angra dos Reis) plot within the olivine + plagioclase field of the Longhi (1999) phase diagram relevant

to angrite petrogenesis and that crystallization starts with these phases, followed by the addition of clinopyroxene crystallization. This is consistent with the evidence we presented earlier of possible crystallization of some olivine and plagioclase before clinopyroxene crystallization in Asuka 881371 (e.g., Fig. 7b). It seems likely that the magmas for the angrites, LEW 87051, Asuka 881371, Sahara 99555 and D'Orbigny, may have come from somewhat different sources, resulting in slightly different bulk major element compositions, but followed similar crystallization sequences, accounting for the basic similarities in their trace element compositional trends. LEW 86010, as noted before, must have a separate origin.

Although we have not discussed Angra dos Reis in detail, we note that Crozaz and McKay (1990) excluded a common magmatic origin for LEW 86010 and Angra dos Reis on the basis of trace element distributions. Pyroxenes from Angra dos Reis have distinctly elevated trace element compositions and low fe# values compared to LEW 86010 pyroxenes. Comparison of Figures 3 and 4 from Crozaz and McKay (1990) with our Figure 5 shows that Angra dos Reis cannot be co-magmatic with the other four angrites either.

5. CONCLUSIONS

We investigated the trace element distributions of the two new angrites, Sahara 99555 and D'Orbigny and compared them with the three Antarctic angrites, LEW 86010, LEW 87051 and Asuka 881371. Four of these angrites (LEW 87051, Asuka 881371, Sahara 99555 and D'Orbigny) are texturally similar and appear to be closely related. Trace element trends in clinopyroxene and olivine show that they crystallized from very similar magmas. Large variations in incompatible trace element concentrations indicate that crystallization was rapid and proceeded under essentially closed system conditions. Discrepancies between bulk REE compositions and the compositions of the melts calculated to be in equilibrium with the major phases are probably due, at least in part, to kinetic effects. Prior crystallization of olivine and/or anorthite may also account for the elevated clinopyroxene parent melt compositions of some of these angrites, such as Asuka 88131.

Rapid crystallization of the angrites is consistent with their textural features, such as the skeletal anorthite crystals and complex intergrowths of olivine and plagioclase seen in Sahara 99555 and D'Orbigny (Mikouchi et al., 2000a; Mikouchi and McKay, 2001), and with crystallization experiments that reproduce their textures and mineralogies (Mikouchi et al., 2000b, 2001). As suggested by these authors, the angrites apparently formed as thin lava flows, probably within 1 m of the surface of the angrite parent body. The more fine-grained textures of LEW 87051 and Sahara 99555 suggest that they may have cooled slightly more rapidly than Asuka 881371 and D'Orbigny. Mikouchi et al. (1996, 2001) suggested impact melting as a plausible heat source for producing these magmas, although endogenous melting and surface eruption are also possible. Our data do not distinguish between these possibilities.

LEW 86010 also crystallized from a melt and appears to represent a liquid composition (e.g., Crozaz and McKay, 1990). However, trace element trends in clinopyroxene are distinctly different from those of the other angrites studied here and, thus, this meteorite must have crystallized from a different source magma.

Acknowledgments—We thank the Meteorite Working Group for the loan of thin sections of LEW 86010 and LEW 87051. We are also grateful to E. Inazaki and T. Smolar for ion microprobe maintenance. We greatly appreciate constructive comments by M. Kimura, A. Treiman and an anonymous reviewer, which improved this manuscipt. This work was supported by NSF grant EAR-9980394 to G. Crozaz.

Associate editor: S. S. Russell

REFERENCES

Alexander C. M. O'D. (1994) Trace element distributions within ordinary chondrite chondrules: Implications for chondrule formation conditions and precursors. *Geochim. Cosmochim. Acta* **58,** 3451–3467.

Anders E. and Grevesse N. (1989) Abundances of the elements: Meteoritic and solar. *Geochim. Cosmochim. Acta* **53,** 197–214.

Bischoff A., Clayton R. N., Markl G., Mayeda T. K., Palme H., Schultz L., Srinivasan G., Weber H. W., Weckwerth G., and Wolf D. (2000) Mineralogy, chemistry, noble gases, and oxygen- and magnesium-isotopic compositions of the angrite Sahara 99555 [abstract]. *Meteorit. Planet. Sci.* **35,** A27.

Crozaz G. and McKay G. (1990) Rare earth elements in Angra dos Reis and Lewis Cliff 86010, two meteorites with similar but distinct magma evolutions. *Earth Planet. Sci. Lett.* **97,** 369–381.

Crozaz G. and Wadhwa M. (2001) The terrestrial alteration of Saharan shergottites Dar al Gani 476 and 489: A case study of weathering in a hot desert environment. *Geochim. Cosmochim. Acta* **65,** 971–978.

Crozaz G., Floss C., and Wadhwa M. (2002) Chemical alteration of hot and cold desert meteorites [abstract]. *Geochim. Cosmochim. Acta* **66,** A158.

Delaney J. S. and Sutton S. R. (1988) Lewis Cliff 86010, an ADORable Antarctican [abstract]. *Lunar Planet. Sci.* **19,** 265–266.

Floss C. and Crozaz G. (1991) Ce anomalies in the LEW85300 eucrite: Evidence for REE mobilization during Antarctic weathering. *Earth Planet. Sci. Lett.* **107,** 13–24.

Floss C. and Jolliff B. (1998) Rare earth element sensitivity factors in calcic plagioclase (anorthite). In *Secondary Ion Mass Spectrometry, SIMS XI* (eds. G. Gillen, R. Lareau, J. Bennett, and F. Stevie), pp. 785–788. John Wiley, New York.

Floss C., Crozaz G., and Mikouchi T. (2000) Sahara 99555: Trace element compositions and relationship to Antarctic angrites [abstract]. *Meteorit. Planet. Sci.* **35,** A53.

Floss C., Killgore M., and Crozaz G. (2001) Trace element compositions and petrogenesis of the D'Orbigny angrite [abstract]. *Lunar Planet. Sci.* **32,** #1201.

Gallahan W. E. and Nielsen R. L. (1992) The partitioning of Sc, Y, and the rare earth elements between high-Ca pyroxene and natural mafic to intermediate lavas at 1 atmosphere. *Geochim. Cosmochim. Acta* **56,** 2387–2404.

Goodrich C. A. (1988) Petrology of the unique achondrite LEW 86010 [abstract]. *Lunar Planet. Sci.* **19,** 399–400.

Grossman J. N. and Zipfel J. (2001) The Meteoritical Bulletin, No. 85, 2001 September. *Meteorit. Planet. Sci.* **36,** A293–A322.

Hsu W. (1995) *Ion Microprobe Studies of the Petrogenesis of Enstatite Chondrites and Eucrites*. Ph.D. dissertation, Washington University.

Jambon A., Barrat J. A., and Boudouma O. (2002) A new angrite from Morocco: Preliminary data [abstract]. *Meteorit. Planet. Sci.* **37,** A71.

Jones J. H. (1995) Experimental trace element partitioning. In *Rock Physics and Phase Relations, a Handbook of Physical Constants* (ed. T. J. Ahrens), pp. 73–104. American Geophysical Union.

Jones R. H. and Layne G. D. (1997) Minor and trace element partitioning between pyroxene and melt in rapidly cooled chondrules. *Am. Mineral.* **82,** 534–545.

Kaneda K., Mikouchi T., Saito A., Sugiyama K., Ohsumi K., Mukai M., Osaka T., Miyata Y., Nakai M., Kasama T., Chikami J., and Miyamoto M. (2001) Mineralogy of unique calcium silico-phosphates in angrites [abstract]. *Lunar Planet. Sci.* **32,** #2127.

Kennedy A. K., Lofgren G. E., and Wasserburg G. J. (1993) An experimental study of trace element partitioning between olivine, orthopyroxene and melt in chondrules: Equilibrium values and kinetic effects. *Earth Planet. Sci. Lett.* **115,** 177–195.

Kurat G., Brandstätter F., Clayton R., Nazarov M. A., Palme H., Schultz L., Varela M. E., Wäsch E., Weber H. W., and Weckwerth G. (2001a) D'Orbigny: A new and unusual angrite [abstract]. *Lunar Planet. Sci.* **32,** #1753.

Kurat G., Varela M. E., Brandstätter F., Wäsch E., and Nazarov M. A. (2001b) D'Orbigny: A new window into angrite genesis [abstract]. *Lunar Planet. Sci.* **32,** #1737.

Kurat G., Ntaflos T., Brandstätter F., Varela M. E., Sylvester P. J., and Nazarov M. A. (2001c) Trace element contents of major phases of the D'Orbigny angrite [abstract]. *Meteorit. Planet. Sci.* **36,** A108.

Longhi J. (1999) Phase equilibrium constraints on angrite petrogenesis. *Geochim. Cosmochim. Acta* **63,** 573–585.

Lugmair G. W. and Marti K. (1977) Sm-Nd-Pu timepieces in the Angra dos Reis meteorite. *Earth Planet. Sci. Lett.* **35,** 273–284.

Lugmair G. W. and Galer S. J. G. (1992) Age and isotopic relationships among the angrites Lewis Cliff 86010 and Angra dos Reis. *Geochim. Cosmochim. Acta* **56,** 1673–1694.

McKay G. A. (1986) Crystal/liquid partitioning of REE in basaltic systems: Extreme fractionation of REE in olivine. *Geochim. Cosmochim. Acta* **50,** 69–79.

McKay G., Lindstrom D., Yang S.-R., and Wagstaff J. (1988a) Petrology of unique achondrite Lewis Cliff 86010 [abstract]. *Lunar Planet. Sci.* **19,** 762–763.

McKay G., Lindstrom D., Le L., and Yang S.-R. (1988b) Experimental studies of synthetic LEW 86010 analogs: Petrogenesis of a unique achondrite [abstract]. *Lunar Planet. Sci.* **19,** 760–761.

McKay G., Crozaz G., Wagstaff J., Yang S.-R., and Lundberg L. (1990) A petrographic, electron microprobe and ion microprobe study of mini-angrite Lewis Cliff 87051 [abstract]. *Lunar Planet. Sci.* **21,** 771–772.

McKay G., Le L., and Wagstaff J. (1991) Olivines in angrite LEW 87051: Phenos or xenos? [abstract]. *Meteoritics* **26,** 370.

McKay G., Le L., Wagstaff J., and Crozaz G. (1994) Experimental partitioning of rare earth elements and strontium: Constraints on petrogenesis and redox conditions during crystallization of Antarctic angrite Lewis Cliff 86010. *Geochim. Cosmochim. Acta* **58,** 2911–2919.

McKay G., Crozaz G., Mikouchi T., and Miyamoto M. (1995a) Petrology of Antarctic angrites LEW 86010, LEW 87051 and Asuka 881371 [abstract]. *Antarct. Meteorites* **20,** 155–158.

McKay G., Crozaz G., Mikouchi T., and Miyamoto M. (1995b) Exotic olivine in Antarctic angrites LEW87051 and Asuka 881371 [abstract]. *Meteoritics* **30,** 543–544.

Mikouchi T, McKay G. (2001) Mineralogical investigation of D'Orbigny: A new angrite showing close affinities to Asuka 881371, Sahara 99555 and Lewis Cliff 87051 [abstract]. *Lunar Planet. Sci.* **32,** #1876.

Mikouchi T., Miyamoto M., and McKay G. A. (1996) Mineralogical study of angrite Asuka-881371: Its possible relation to angrite LEW 87051. *Proc. NIPR Symp. Antarct. Meteorites* **9,** 174–188.

Mikouchi T., McKay G., Le L., and Mittlefehldt D. W. (2000a) Preliminary examination of Sahara 99555: Mineralogy and experimental studies of a new angrite [abstract]. *Lunar Planet. Sci.* **31,** #1970.

Mikouchi T., McKay G. A., and Le L. (2000b) Experimental crystallization of the Asuka 881371 (angrite) groundmass composition: Implications for crystallization histories of Sahara 99555 [abstract]. *Meteorit. Planet. Sci.* **35,** A110–A111.

Mikouchi T., Miyamoto M., McKay G., and Le L. (2001) Cooling rate estimates of quenched angrites: Approaches by crystallization experiments and cooling rate calculations of olivine xenocrysts [abstract]. *Meteorit. Planet. Sci.* **36,** A134–A135.

Mittlefehldt D. W. and Lindstrom M. M. (1990) Geochemistry and genesis of the angrites. *Geochim. Cosmochim. Acta* **54,** 3209–3218.

Mittlefehldt D. W. and Lindstrom M. M. (1991) Generation of abnormal trace element abundances in Antarctic eucrites by weathering processes. *Geochim. Cosmochim. Acta* **55,** 77–87.

Mittlefehldt D. W., McCoy T. J., Goodrich C. A., and Kracher A. (1998) Non-chondritic meteorites from asteroidal bodies. In *Planetary Materials* (ed. J. J. Papike), p. 195. Mineralogical Society of America, Washington, DC.

Mittlefehldt D. W., Killgore M., and Lee M. T. (2002) Petrology and geochemistry of D'Orbigny, geochemistry of Sahara 99555, and the origin of angrites. *Meteorit. Planet. Sci.* **37,** 345–369.

Nyquist L. E., Bansal B., Wiesmann H., and Shih C.-Y. (1994) Neodymium, strontium and chromium isotopic studies of the LEW86010 and Angra dos Reis meteorites and the chronology of the angrite parent body. *Meteoritics* **29,** 872–885.

Premo W. R. and Tatsumoto M. (1995) Pb isotopic systematics of angrite Asuka-881371 [abstract]. *Antarct. Meteorites* **20,** 204–206.

Prinz M. and Weisberg M. K. (1995) Asuka 881371 and the angrites: Origin in a heterogeneous, CAI-enriched, differentiated, volatile-depleted body [abstract]. *Antarct. Meteorites* **20,** 207–210.

Prinz M., Keil K., Hlava P. F., Berkley J. L., Gomes C. B., and Curvello W. S. (1977) Studies of Brazilian meteorites, III. Origin and history of the Angra dos Reis achondrite. *Earth Planet. Sci. Lett.* **35,** 317–330.

Prinz M., Weisberg M. K., and Nehru C. E. (1990) LEW 87051, a new angrite: Origin in a Ca-Al-enriched eucritic planetesimal [abstract]. *Lunar Planet. Sci.* **21,** 979–980.

Störzer D. and Pellas P. (1977) Angra dos Reis: Plutonium distribution and cooling history. *Earth Planet. Sci. Lett.* **35,** 285–293.

Treiman A. H (1989) An alternate hypothesis for the origin of Angra dos Reis: Porphyry, not cumulate. In *Proc. 19th Lunar Planet. Sci. Conf.*, pp. 443–450.

Varela M. E., Kurat G., Brandstätter F., Bonnin-Mosbah M., and Metrich N. (2001a) Glasses in the D'Orbigny angrite [abstract]. *Lunar Planet. Sci.* **32,** # 1803.

Varela M. E., Kurat G., Ntaflos T., Brandstätter F., and Sylvester P. J. (2001b) Trace elements in glass of the D'Orbigny angrite [abstract]. *Meteorit. Planet. Sci.* **36,** A211.

Warren P. and Davis A. M. (1995) Consortium investigation of the Asuka-881371 angrite: Petrographic, electron microprobe, and ion microprobe observations [abstract]. *Antarct. Meteorites* **20,** 257–260.

Warren P. H., Kallemeyn G. W., and Mayeda T. (1995) Consortium investigation of the Asuka-881371 angrite: Bulk-rock geochemistry and oxygen isotopes [abstract]. *Antarct. Meteorites* **20,** 261–264.

Wasserburg G. J., Tera F., Papanastassiou D. A., and Huneke J. C. (1977) Isotopic and chemical investigations on Angra dos Reis. *Earth Planet. Sci. Lett.* **35,** 294–316.

Yanai K. (1994) Angrite Asuka-881371: Preliminary examination of a unique meteorite in the Japanese collection of Antarctic meteorites. *Proc. NIPR Symp. Antarct. Meteorites* **7,** 30–41.

Zinner E. and Crozaz G. (1986a) A method for the quantitative measurement of rare earth elements in the ion microprobe. *Intl J. Mass Spec. Ion Proc.* **69,** 17–38.

Zinner E. and Crozaz G. (1986b) Ion probe determination of the abundances of all the rare earth elements in single mineral grains. In *SIMS V* (eds. A. Benninghoven, R. J. Colton, D. S. Simons, and H. W. Werner), pp. 444–446. Springer-Verlag, New York.